PROCEEDINGS OF SPIE

SPIEDigitalLibrary.org/conference-proceedings-of-spie

Nano-Raman spectral imaging of localized vibrations in two-dimensionais systems

Ado Jorio, Cassiano Rabelo, Rafael Nadas, Hudson Miranda, Thiago Vasconcelos, et al.

Ado Jorio, Cassiano Rabelo, Rafael Nadas, Hudson Miranda, Thiago Vasconcelos, Bráulio S. Archanjo Sr., Andreij C. Gadelha, Luiz Gustavo Cançado, "Nano-Raman spectral imaging of localized vibrations in two-dimensionais systems," Proc. SPIE 12203, Enhanced Spectroscopies and Nanoimaging 2022, 1220302 (3 October 2022); doi: 10.1117/12.2633265

SPIE.

Event: SPIE Nanoscience + Engineering, 2022, San Diego, California, United States

Invited Paper

Nano-Raman spectral imaging of localized vibrations in two-dimensionais systems

Ado Jorio*[a], Cassiano Rabelo[a], Rafael Nadas[a], Hudson Miranda[a], Thiago Vasconcelos[b], Bráulio S. Archanjo[b], Andreij C. Gadelha [a,c], Luiz Gustavo Cançado[a]
[a]Universidade Federal de Minas Gerais, Belo Horizonte, MG, Brazil 31270-901; [b]Divisão de Metrologia de Materiais, Inmetro, Duque de Caxias, RJ, Brazil CEP; [c]Present address: Univ. Colorado, Boulder, CO, USA ZIP

ABSTRACT

Here we report graphene systems' nano-Raman hyperspectral imaging based on tip-enhanced Raman scattering (TERS). The vibrational and electronic structures are modulated within the graphene-related materials, leading to nano-scale changes in the behavior of electrons and phonons that can be used for spectral imaging. Furthermore, we utilize a He-focused ion beam to do nanolithography on graphene. We then show that the tiny features on graphene made by the He-focused ion beam can only be visualized under nanometer-scaled spectroscopy imaging. We have also imaged low-angle reconstructed twisted bilayer graphene, and our observations highlight the relevance of solitons and topological points for the structures' vibrational and electronic properties, relevant in the context of twistronics.

Keywords: Tip-enhanced Raman spectroscopy, nano-Raman spectroscopy, spectral imaging, twisted bilayer graphene, electrons, phonons

1. INTRODUCTION

Figure 1 shows how our perception of nature depends on our ability to distinguish details of a given object. While a field, a flower, and a bee, as shown in panels (a-c), can be seen with naked eyes, the structural details of the bee's eye, including its cells and hair, as shown in panel (d), can only be visualized with the help of an optical microscope. However, to go beyond the figure in panel (d), a nanoscope able to surpass the diffraction limit of visible light is necessary.

Figure 1. (a-d) are images from a flower field on different levels of magnification, focusing on a flower and bee (b), on a bee (c) and on the eye of the bee (d). (a-c) are visible with naked eye, while (d) requires an optical microscope.

Enhanced Spectroscopies and Nanoimaging 2022, edited by Prabhat Verma, Yung Doug Suh,
Proc. of SPIE Vol. 12203, 1220302 · © 2022 SPIE ·
0277-786X · doi: 10.1117/12.2633265

The limit of spatial resolution in optics arises from the occurrence of non-propagating near-field components of light. The lack of information spoils the proper observation of tiny structural details of the object under analysis. More precisely, features that are smaller than half-wavelength of the light cannot be reconstructed from the image formed at the detection plane. As such, although conventional optical microscopy and spectroscopy have been developed for more than 500 years, their use for studying nanomaterials is limited. Waves of matter (electrons) with wavelengths in the sub-nanometer scale provided an alternative to work around the problem, and the first crystal lattice was directly observed in the early fifties by field ion microscopy, FIM[1,2]. Atomic resolution was achieved in 1970 with scanning transmission electron microscopy, STEM[3], and individual atoms were imaged in 1983 by scanning tunneling microscopy, STM[4]. These electron-based alternatives, however, lack the valuable information that can be carried out by the interaction of matter with light, in the vast framework of optical spectroscopy. Here we focus on tip-enhanced Raman spectroscopy (TERS)[5], which provides nano-scale resolution and chemical information from the materials. It will be shown how this technique has made it possible to generate optical images of crystal superlattices[6]. In TERS, the images resemble spectral variations which can be used for investigation of materials properties at the nanoscale by means of optical microscopy[7].

2. METHODS

Nano-Raman spectroscopy is achieved by coupling a micro-Raman spectrometer to a plasmonic nanoantenna controlled by a tuning fork-based scanning probe microscope[8]. Figure 2 exhibits the structure of the TERS tip utilized in our setup. Panel (a) displays the macroscopic structure of a tuning fork soldered to a tip-holder utilized for tip-replacement in the system, which is a *Porto SNOM* from FabNS. The structure highlighted in (a) with a red-dashed rectangle is zoomed in panel (b), which shows a scanning electron microscope (SEM) image of the plasmon-tunable tip pyramid (PTTP)[9,10] attached to the end of the tuning fork. Panels (c) and (d) are two other SEM images of the TERS tip, at higher magnification, evidencing the presence of a nanometer-sized pyramidal tip and the top of a plateau in the micrometer-sized tip. The PTTP is a nanofabricated TERS antenna[11]. Its nanopyramid tip can be size-adjusted to match the localized surface plasmon resonance wavelength to the laser wavelength. Thus, optimal Raman signal enhancements combined with ~20 nm resolution TERS images are generated, as described in Ref. 10. Recently, PTTP tips have been demonstrated to generate up to two orders of magnitude TERS enhancement factors, generating excellent two-dimensional systems images[6,7,12].

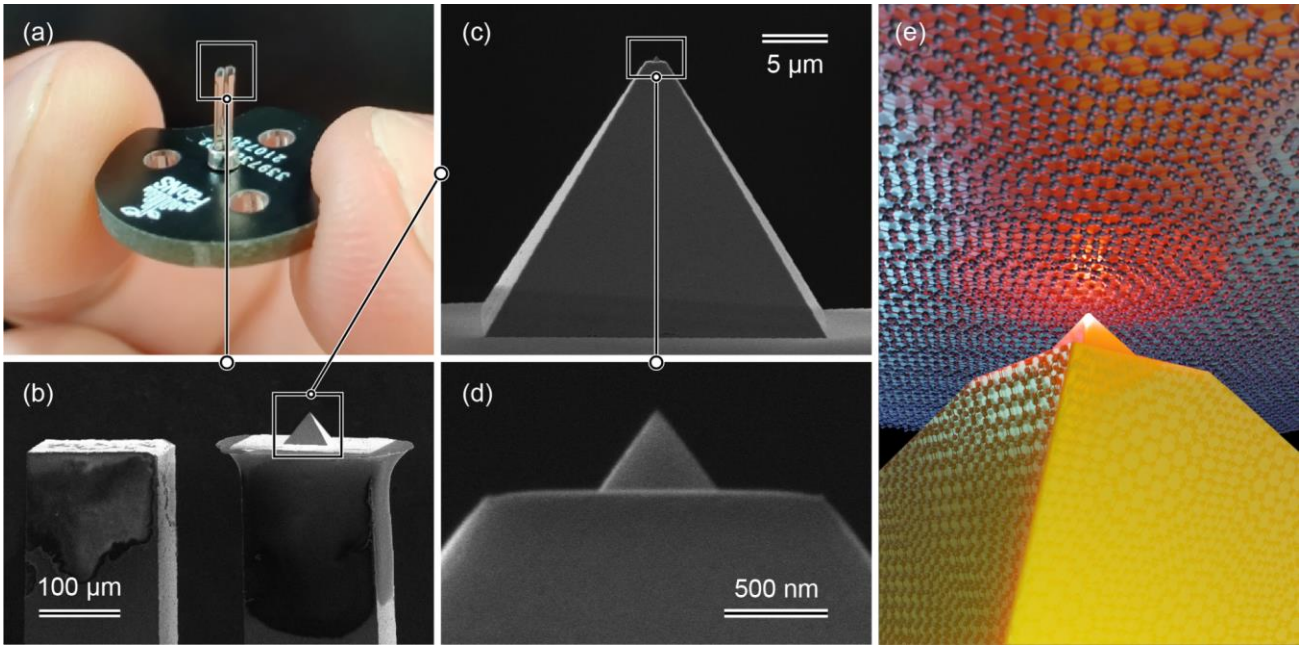

Figure 2. Details of a TERS tip named PTTP mounted on a quartz tuning fork fitted on a magnetically coupled device which allows for friendly probe exchange. (b) is a SEM image zooming the rectangle area marked in the optical image (a). (c,d) are SEM images of the PTTP with higher magnification, both images adapted from Ref. 10. (e) is a schematic representation of the TERS tip, under a glass coverslip containing a TBLG sample, being illuminated by a focused red laser, adapted from Ref. 6.

3. RESULTS

Two defect patterns on graphene samples were produced with Helium Ion Microscopy (HIM) to demonstrate the TERS image resolution and analysis capacity. The patterns were imaged by both micro-Raman and TERS (see Fig. 3), following the method reported in reference[9]. A He^+-focused ion beam with a low dose (1 × 1016 ions/nm^2) was applied to create the nano-sized defective features. The first pattern, shown in Figs. 3(a-d), reproduces the logo of the Federal University of Minas Gerais (UFMG, standing for *Universidade Federal de Minas Gerais*) on a single-layer graphene sheet. While Figs. 3(a,b) were recorded in a conventional hyperspectral Raman imaging system, Figs. 3(c,d) were obtained using the TERS resource. As can be clearly seen, this ~3 μm sized pattern has details in the nanometer scale which cannot be accessed by a conventional optical system. Indeed, as shown in Figs. 3(a,b), the patterned characters are blurred and cannot be read when the ordinary hyperspectral Raman image is recorded. On the other hand, the corresponding TERS images shown in Figs. 3(c,d) highlight the nanometer-scale details, and the UFMG's logo becomes clear.

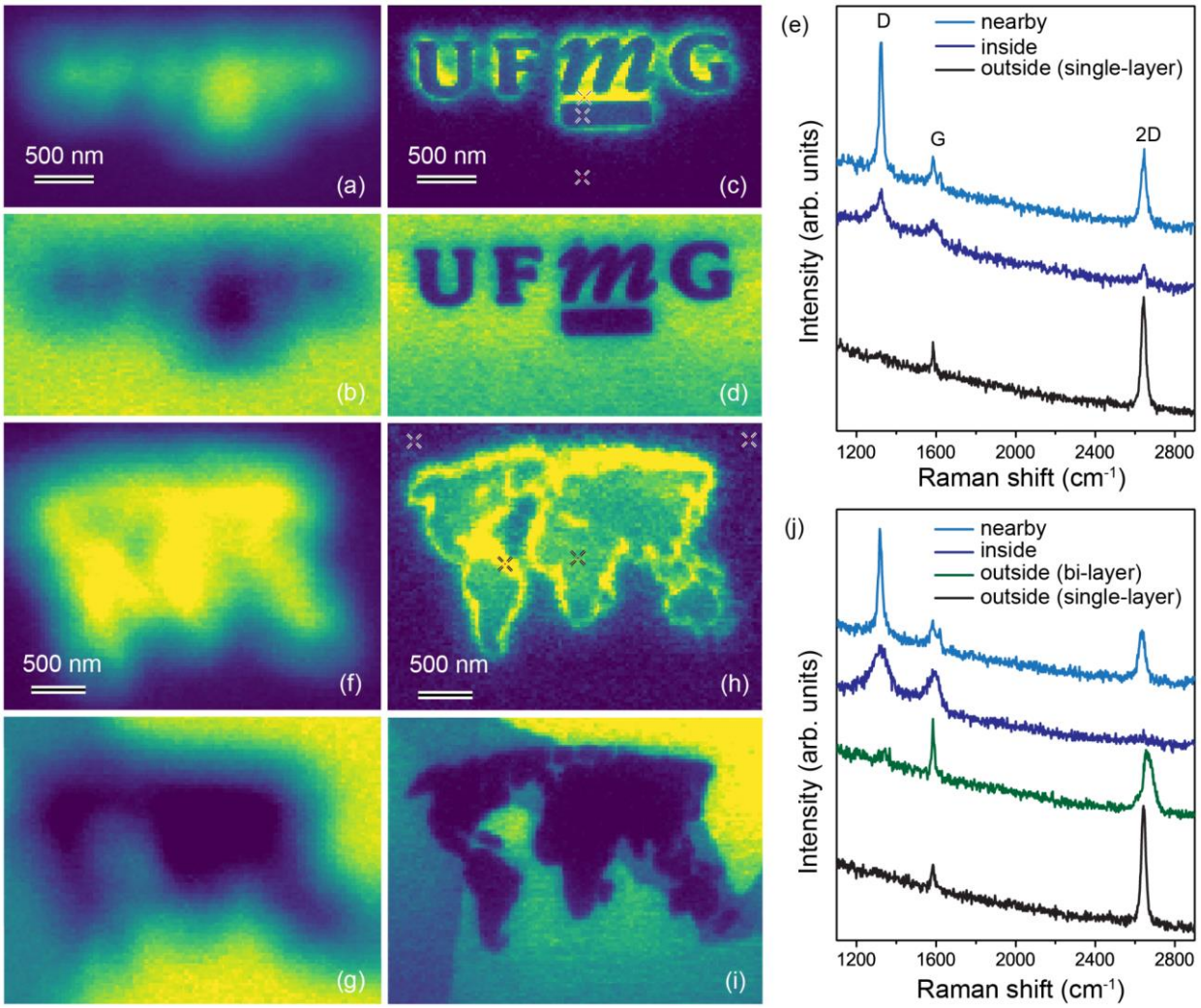

Figure 3. (a,b,f,g) micro-Raman and (c,d,h,i) TERS hyperspectral images of two HIM-patterned graphene samples (UFMG's logo and world map). The color scale stands for the intensity of the defect-induced D band in (a,c,f,h), and for the intensity of the 2D band in (b,d,g,i). The micro-Raman image was produced with 0.2 s of integration time per pixel and 3.3 mW of laser power, and the TERS image was produced with 0.3 s of integration time per pixel and 330 μW of laser power. (e) TERS spectra acquired nearby (light blue), inside (dark blue) and outside (black) the "UFMG" patterned characters. (j) TERS spectra nearby (light blue), inside (dark blue) and outside (at bi-layer region – dark gray, at single-layer region – black) the world map pattern. The × symbols in panels (c) and (h) pinpoint the positions where TERS spectra were acquired.

TERS hyperspectral images also provide extensive chemical and structural information. For example, the color scales in Figs. 3(c,d) render the defect-induced D band (centered at ∼1350 cm−1) and the 2D band (centered at ∼2700 cm^{-1}). Figure 3(f) shows three spectra selected from distinct points (inside/nearby/outside the patterns, as indicated by the arrows in panel (c)). These spectra indicate that HIM produced strong amorphization of the graphene lattice inside the defective regions, induced relatively mild defective sites in the surrounding area, and did not affect regions far from the pattern. A similar analysis is shown in Figures 3(f-i), which present micro-Raman 3(f,g) and TERS 3(h,i) hyperspectral images of the world map. The information contained in TERS images shown in Figures 3(h,i), and also in the spectra shown in Fig. 3(j), indicates that the pattern was drawn on top of a half-single-layer/half-bi-layer graphene flake, generating amorphization in the middle of the patterned area, and soft-induced defective sites nearby.

Two-dimensional systems provide an excellent platform for TERS hyperspectral imaging[6,7,9,12]. Gate-induced homojunctions can be formed and imaged in graphene and MoS_2.[12] On the other hand, twisted bilayer graphene undergoes a self-organized lattice reconstruction, leading to the formation of a periodically repeated domain, which can be observed in TERS experiments[6]. Furthermore, the vibrational and electronic structures are modulated within the material, leading to changes in the behavior of electron-phonon coupling[6]. Our observations highlight the relevance of solitons and topological points for the vibrational and electronic properties of the structures, particularly for small twist angles. They represent a step towards understanding the pertinence of electron-phonon interaction in these systems, relevant in the context of twistronics. Technical details about sample preparation and characterization are discussed in references[6,13].

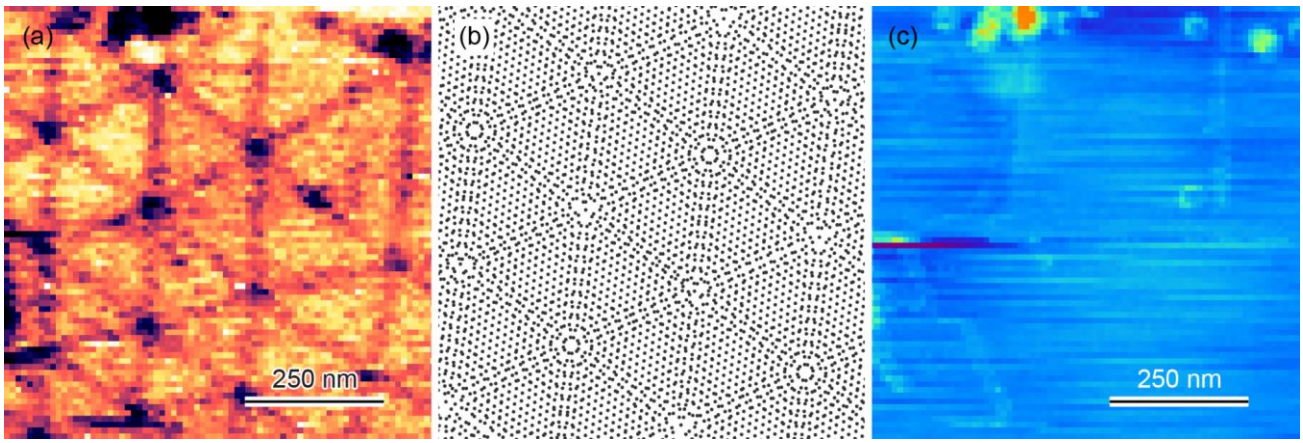

Figure 4. Images of low-angle reconstructed twisted bilayer graphene: (a) TERS; (b) schematics; (c) topography (AFM) ate the same location as (a). (a,c) adapted from Ref. 6.

Figs. 4(a-c) show three images of low-angle reconstructed twisted bilayer graphene. Panel (a) is a TERS image based on the 2D band intensity[6]. A schematic image of the atomic structure corresponding to panel (a) that considers a rotation angle $\theta = 0.8^{o}$ and the reconstruction of AB and BA sites is shown in panel (b). Panel (c) exhibits a topography image obtained from atomic force microscopy (AFM), where the AB-BA domain walls and the AA stacked regions are not observed. We only observe contamination features in the AFM image, which are also present in the TERS image. As stated in the introduction, this was the first optical observation of a crystal lattice, a remarkable achievement considering that optical microscopy has been under development for at least five centuries.

4. CONCLUDING REMARKS

Nano-Raman spectroscopy based on a tip-enhanced Raman spectrometer is a valuable tool for two-dimensional imaging systems. It allows nanoscale observation of the materials and provides deep insight into their quantum properties. The

technique's success depends on reliable and efficient TERS tips, and the tip named PTTP, standing for plasmon-tunable tip pyramid, provide a good solution both for fabrication[9,10], based on broadly developed silicon patterning technology, and for unprecedented enhancement efficiency, due to the specificities of the tip shape[14].

*adojorio@fisica.ufmg.br; phone +55 31 3409-6612; fax +55 31 3409-5600; labns.com.br

REFERENCES

[1] Müller, E. W. and Bahadur, K. Phys. Rev. 102, 624-631 (1956)
[2] Müller, E. W., J. of Appl. Phys. 27, 474-476 (1956)
[3] Crewe, A. V., Wall J. and Langmore, J. Science 168(3937), 1338-1340 (1970)
[4] Binnig, G., Rohrer, H., Gerber, Ch. and Weibel E. Phys. Rev. Lett. 50, 120-123 (1983)
[5] Costa, M. D. D., Cançado, L. G., Jorio, A. Journal of Raman Spectroscopy 52 (3), 587-599 (2021)
[6] Gadelha, A. C., et al. Nature 590 (7846), 405-409 (2021)
[7] Malard, L. M., et al. Physical Chemistry Chemical Physics 23 (41), 23428-23444 (2021)
[8] Rabelo, C. et al. Proceedings of the 4th International Symposium on Instrumentation Systems, Circuits and Transducers (INSCIT), 2019, Sao Paulo. p. 1
[9] Vasconcelos, T. L., et al. IEEE Journal of Selected Topics in Quantum Electronics 27 (1), 1-11 (2021)
[10] Vasconcelos, T. L., et al. Advanced Optical Materials 6 (20), 1800528-1800534 (2018)
[11] Bruno S. Oliveira, et al., The Journal of Chemical Physics 153 (11) 114201-114208 (2020)
[12] Gadelha, A. C., et al. The Journal of Physical Chemistry Letters 12 (31), 7625-7631 (2021)
[13] Gadelha, A. C., et al. ACS Applied Nanomaterials 4 (2), 1858-1866 (2021)
[14] Hudson, M. et al. Physica Status Solidi-Rapid Research Letters, 2000212 (2020)